LA-UR-81-1811

TITLE: THEORETICAL MODEL OF LIQUID METALS

AUTHOR(S): Gerald I. Kerley

SUBMITTED TO: To be presented at the 8th Thermophysical Properties Conference, NBS, Gaithersburg, MD, 15-18 June.

MASTER

University of California

LOS ALAMOS SCIENTIFIC LABORATORY

Post Office Box 1663 Los Alamos, New Mexico 87545

An Affirmative Action / Equal Opportunity Employer

Form No. 836 R3
St. No. 2629
12/78

UNITED STATES
DEPARTMENT OF ENERGY
CONTRACT W-7405-ENG. 36

THEORETICAL MODEL OF LIQUID METALS*

G. I. Kerley

Theoretical Division, Los Alamos National Laboratory
Los Alamos, NM 87545

ABSTRACT

A theory for calculating the bulk properties of metals and other materials is described. The approach is based upon the fluid perturbation theory of Kerley [1-3] and the electronic structure model of Liberman [4]. Application of the theory involves three steps. First, the zero Kelvin isotherm of the solid is constructed from electronic structure calculations, experimental data, or both. This curve contains information about the effective interactions between atoms in the ground electronic state. Next, the cold curve is combined with perturbation theory to compute contributions from thermal motion of the atoms to the liquid properties. Finally, contributions from thermal electron excitation are computed using the electronic structure model. In this paper, we show that theory agrees well with experimental data for xenon and iron.

INTRODUCTION

Because of recent progress in the theory of fluids [5,6], it is now possible to make accurate calculations of the equation of state (EOS) and other bulk properties starting with specified intermolecular forces. However, attempts to apply the new theories to specific materials are hampered by lack of knowledge about the interaction potentials. Calculations for liquid metals are particularly complicated because the effective potentials depend upon density [7].

For this reason, we have developed a theory of fluids [1-3], called the CRIS model, that does not require explicit knowledge of the intermolecular potentials. Instead, the potential energy of a fluid molecule in the cage formed by its neighbors is calculated from the zero Kelvin isotherm (cold curve) of the solid. While doing away with the pair potential, the theory retains the essential features of a fluid model, and it agrees well with results from computer experiments for simple potentials [3]. Since the solid cold curve is often known from either theory or experiment, the model can be applied to many practical problems.

In the CRIS model, the electrons are taken to be in the ground state. In this paper, we use the average atom model of Liberman [4] to calculate additional contributions to the EOS from thermal excitation of the electrons. These terms are essential for describing metals with a high electronic specific heat and for explaining very high pressure shock wave data in rare gases and other materials.

DESCRIPTION OF THE MODELS

Two computer programs were used in our calculations. The PANDA code [8] computes the pressure, internal energy, and Helmholtz free energy, as functions of density and temperature, for both solid and liquid phases; the melting line is located by matching the pressures and Gibbs free energies of the two phases as a function of temperature. The INFERNO code [9] computes the thermal electronic contributions to the EOS, which are

input to PANDA. Our description of these models and codes will be brief. Details are discussed in Refs. 1-4 and 8.

The Solid Model

For the cases considered in this paper, the solid EOS can be written as the sum of three terms. For example, the pressure is given by

$$P_S(\rho,T) = P_C(\rho) + P_L(\rho,T) + P_E(\rho,T), \qquad (1)$$

where ρ is the density and T is the temperature. Formulas for the energy and free energy are similar to Eq. (1).

$P_C(\rho)$ is the electronic contribution to the zero Kelvin isotherm, which we have constructed using both theoretical methods and experimental data. For xenon, as discussed below, we used the a priori calculations of Ross and McMahan [10]. For iron, we used the measurements of Mao and Bell [11].

$P_L(\rho,T)$ is the lattice vibrational contribution to the EOS. We use the Debye model,

$$P_L(\rho,T) = \frac{R}{W}\gamma\rho\left[\frac{9}{8}\theta + \frac{9T^4}{\theta^3}\int_0^{\theta/T}\frac{x^3}{e^x-1}dx\right]. \qquad (2)$$

R is the gas constant, W is the molecular weight, θ is the Debye temperature, and γ is the Grüneisen function. The density dependence of γ and θ were determined from a formula like that of Slater [12], but adjusted to agree with experimental data at the normal solid density [8].

$P_E(\rho,T)$ is the thermal electronic contribution to the EOS, which is discussed below.

The Fluid Model

The EOS for the fluid phase consists of two terms. The pressure is given by

$$P_F(\rho,T) = P_N(\rho,T) + P_E(\rho,T). \qquad (3)$$

$P_N(\rho,T)$ includes contributions from the ground electronic state and the nuclear degrees of freedom, calculated using the CRIS model, and $P_E(\rho,T)$ is the thermal electron term.

In the CRIS model [2], a function ϕ is defined to be the potential energy of a fluid atom in the cage of its neighbors. The structure of this cage and the energy ϕ vary from molecule to molecule. The fluid properties are computed using a perturbation expansion which involves averages of ϕ over the appropriate distribution function. To first order, the Helmholtz free energy is

$$\tilde{A}_N(\rho,T;\sigma) = A_0(\rho,T;\sigma) + N\langle\phi\rangle_0 . \qquad (4)$$

Here A_0 is the free energy of a hard sphere fluid, σ is the hard sphere diameter, N is the total number of molecules, and $\langle\phi\rangle_0$ is an average of ϕ over the hard sphere distribution. σ is defined as a function of density and temperature by minimizing $\tilde{A}_N$. The CRIS model also includes corrections to the first order approximation.

The function ϕ is obtained from the zero Kelvin curve that is constructed for the solid as described above. Hence, $P_N(\rho,T)$ includes contributions from both nuclear and electronic degrees of freedom, with the electrons taken to be in the ground state. However, the nuclear and electronic motions are strongly coupled, so that separate cold curve and nuclear terms cannot be defined as they can for the solid phase.

The Electronic Model

INFERNO, a model for calculating the electronic structure of dense matter, has been developed by Liberman [4]. He considers an average atom, at the center of a Wigner-Seitz sphere, surrounded by an electron gas and a uniform positive charge which simulate the neighboring atoms. He solves the Dirac equation to obtain wave functions and energies for both discrete bound states and continuum free states. The average electron charge density is computed from the wave functions, by populating the energy levels according to Fermi statistics. The screened potential and the charge distribution, which depend upon density and temperature, are required to be self-consistent. The electronic entropy is also calculated from Fermi statistics; the PANDA code computes the pressure, energy, and free energy numerically, using well known thermodynamic formulas.

Calculations using INFERNO exhibit atomic shell structure effects which can cause interesting results in the EOS. In Fig. 1, we compare calculations for aluminum with those using the simpler Thomas-Fermi-Dirac (TFD) theory [9,13]. At low densities, the entropy vs temperature curves exhibit steps which correspond to different stages of ionization. At higher densities this structure disappears because the discrete atomic levels become pressure ionized and broadened into bands. At very high densities, INFERNO and TFD calculations are in good agreement.

XENON - AN A PRIORI CALCULATION

Very high pressure shock wave data for argon and xenon show interesting behavior that appears to be associated with thermal excitation of the electrons. For xenon, it is possible to make an *a priori* calculation and to compare the results with experiment as a test of the theory.

The cold curve used in our work was taken from the band theoretical calculations of Ross and McMahan [10]. We used the INFERNO code to extend their data to higher pressures. The result is shown in Fig. 2. The theoretical cold curve is in good agreement with the experimental data of Syassen and Holzapfel [14].

Like all materials, the rare gases are expected to become metallic at high densities [15]. For xenon, the band calculations [10] predict the energy gap between the filled 5p band and the empty conduction band to close at a density of about 12 g/cc. At the high temperatures reached in the shock wave experiments, effects of the insulator-metal transition can be observed at lower densities. As shown by Ross [15], narrowing of the band gap increases the energy absorbed by electronic excitation and also makes a negative contribution to the pressure; both effects soften the Hugoniot.

The INFERNO calculations give results similar to those predicted by Ross's model. As shown in Fig. 3, the thermal electronic pressure $P_E(\rho,T)$ is negative in the density range 2 - 10 g/cc, for temperatures less than 3 eV. INFERNO predicts closing of the band gap to occur at about 10 g/cc, in fair agreement with the band calculations.

The Hugoniot for xenon [16,17] is shown in Fig. 4. Calculations in which no electronic excitation is allowed are in good agreement with experiment at pressures below 40 GPa but give poor results at the high pressures. When the TFD model is used to describe the electronic excitations, the results are better but still not satisfactory. Calculations using the INFERNO model are in excellent agreement with the experimental data. The theory gives similar results when applied to shock wave data for argon.

IRON

Application of the theory to iron is complicated by the existence of several solid phases. In this study, we have treated iron as if it had only one solid phase, taken to be close-packed. For the purposes of this paper, differences between the hcp ε-phase and the fcc γ-phase are negligible. A more complete EOS calculation, that includes treatment of the bcc α-phase, will be discussed elsewhere.

Experimental and theoretical data [11,18,19] for the cold curve of close packed iron are depicted in Fig. 5. In this work we have used an analytic fit to the data, primarily determined by the measurements of Mao

and Bell [11]. For the solid model, values for the Grüneisen parameter and Debye temperature were taken from Refs. 20 and 21.

In relating the properties of a fluid to the solid cold curve, key assumptions of the CRIS model are that the fluid structure is dominated by short-range forces and that these forces are similar in both the fluid and the solid. In Fig. 6, we compare our calculated structure factor for molten iron with the measurements of Waseda and Suzuki [22]. The agreement is very good, demonstrating that the model gives a good description of the short range liquid structure.

In perturbation theories of fluids, the effective hard sphere diameter σ characterizes the structure and the interaction at short distances. According to Dymond and Alder [23], σ can be used to make a rough estimate of transport properties. The viscosity for molten iron is shown in Fig. 7. The solid curve was calculated from the hard sphere formula [24], using the hard sphere diameter computed from the CRIS model. Agreement with the data of Cavalier [25] is fairly good.

The theoretical melting curve for iron is shown in Fig. 8. In this calculation, we forced agreement with the experimental melting point at zero pressure [26] by subtracting an empirically-determined constant from the free energy of the fluid. This correction was found to be 4.25 kcal/mole, about 4% of the solid binding energy.

Calculated Hugoniots for iron of two initial densities are also shown in Fig. 8. Alpha-phase iron, having a density of 7.85 g/cc, transforms to the ε-phase at about 13 GPa under shock loading [21]. According to our calculations, melting should begin at about 320 GPa. This result is in fair agreement with the value of 260 GPa obtained by Brown and McQueen [20]. Porous α-phase iron, with an initial density of 4.8 g/cc, is predicted to melt at 45 GPa.

Shock velocity-particle velocity curves for iron of various initial densities [20,27,28] are shown in Fig. 9. Agreement between the theory and the measurements for normal density iron is very good over the entire range of the close-packed solid and fluid phases, extending up to 1000 GPa. The theory also predicts the correct behavior as a function of porosity. More detail can be seen in Fig. 10, which shows the shock data for an initial density of 4.8 g/cc. Agreement with experiment is excellent except at the lowest pressures, for which the shocked state is the α-phase.

ACKNOWLEDGEMENT

The author is grateful to D. A. Liberman for assistance in running the INFERNO code.

REFERENCES

* Supported by the U. S. Department of Energy, Division of Basic Energy Sciences.

1. G. I. Kerley, "Perturbation Theory and the Thermodynamic Properties of Fluids. I. General Theory," J. Chem. Phys. 73, 469 (1980).

2. G. I. Kerley, "Perturbation Theory and the Thermodynamic Properties of Fluids. II. The CRIS Model," J. Chem. Phys. 73, 478 (1980).

3. G. I. Kerley, "Perturbation Theory and the Thermodynamic Properties of Fluids. III. Inverse-Power and 6-12 Potentials," J. Chem. Phys. 73, 487 (1980).

4. D. A. Liberman, "Self-Consistent Field Model for Condensed Matter," Phys. Rev. B 20, 4891 (1980).

5. J. A. Barker and D. Henderson, "What is Liquid ? Understanding the States of Matter," Rev. Mod. Phys. 48, 587 (1976).

6. Y. Rosenfeld and N. W. Ashcroft, "Theory of Simple Classical Fluids: Universality in the Short-Range Structure," Phys. Rev. A 20, 1208 (1979).

7. H. D. Jones, "Theory of the Thermodynamic Properties of Liquid Metals," Phys. Rev. A 8, 3215 (1973).

8. G. I. Kerley, "Users Manual for PANDA: a Computer Code for Calculating Equations of State," Los Alamos National Laboratory Report LA-8833-M (1981). (in press)

9. D. A. Liberman, Los Alamos National Laboratory (unpublished).

10. M. Ross and A. K. McMahan, "Condensed Xenon at High Pressure," Phys. Rev. B 21, 1658 (1980).

11. H. K. Mao and P. M. Bell, "Equations of State of MgO and c Fe Under Static Pressure Conditions," J. Geophys. Res. 84, 4533 (1977).

12. J. C. Slater, Introduction to Chemical Physics (McGraw-Hill, New York, 1979).

13. R. D. Cowan and J. Ashkin, "Extension of the Thomas-Fermi-Dirac Statistical Theory of the Atom to Finite Temperatures," Phys. Rev. 105, 144 (1957).

14. K. Syassen and W. B. Holzapfel, "High-Pressure Equation of State for Solid Xenon," Phys. Rev. B 18, 5826 (1978).

15. M. Rose, "Shock Compression of Argon and Xenon. IV. Conversion of Xenon to a Metal-Like State," Phys. Rev. 171, 777 (1968).

16. M. van Thiel, "Compendium of Shock Wave Data," Lawrence Livermore Laboratory Report UCRL-50108 (1977).

17. W. J. Nellis, M. van Thiel, A. C. Mitchell, and M. Ross, "The Equation of State of D_2 and Xe in the Megabar Pressure Range," this conference.

18. M. S. T. Bukowinski, "A Theoretical Equation of State for the Inner Core," Phys. Earth Planet. Interiors 14, 333 (1977).

19. E. A. Kmetko, Los Alamos National Laboratory, unpublished band theoretical calculations.

20. J. M. Brown, and R. G. McQueen, "Thermodynamic Properties for Shocked Porous Iron," J. Geophys. Res., to be published.

21. D. J. Andrews, "Equation of State of the Alpha and Epsilon Phases of Iron," J. Phys. Chem. Solids 34, 825 (1973).

22. Y. Waseda and K. Suzuki, "Atomic Distribution and Magnetic Moment in Liquid Iron by Neutron Diffraction," Phys. Stat. Sol. 39, 669 (1970).

23. J. H. Dymond and B. J. Alder, "Van der Waals Theory of Transport in Dense Fluids," J. Chem. Phys. 45, 2061 (1966).

24. J. H. Dymond, "Corrected Enskog Theory and the Transport Coefficients of Liquids," J. Chem. Phys. 60, 969 (1974).

25. G. Cavalier, "Mesure de la Viscosité du Fer, du Cobalt, et du Nickel," Compt Rend. 256, 1308 (1963).

26. H. M. Strong, R. E. Tuft, and E. E. Hanneman, "The Iron Fusion Curve and γ-δ-ℓ Triple Point," Metall. Trans. 4, 2657 (1973).

27. S. P. Marsh, LASL Shock Hugoniot Data (University of California, Berkeley, 1980).

28. L. Y. Altshuler, N. N. Kalitkin, L. V. Kuzmina, and B. S. Chekin, "Shock Adiabats for Ultrahigh Pressures," Sov. Phys. JETP 45, 167 (1977). Also see Ref. 16.

FIGURE CAPTIONS

Fig. 1. Electronic entropy for aluminum as a function of temperature at several densities. Solid lines were calculated using the INFERNO model, dashed lines were calculated using the TFD model.

Fig. 2. Zero Kelvin isotherm for xenon. Circles are from Ref. 10, squares are from Ref. 14, and triangles were calculated using the INFERNO model. The solid line is the cold curve used in this work.

Fig. 3. Thermal electronic pressure, as a function of density, for xenon at several temperatures.

Fig. 4. Hugoniot data and theoretical calculations for xenon. Squares are from Ref. 16, circles are from Ref. 17.

Fig. 5. Zero Kelvin isotherm for iron. Circles are from Ref. 11, triangles are from Ref. 18, squares are from Ref. 19, and diamonds were calculated using the INFERNO model. The solid line is the cold curve used in this work.

Fig. 6. Structure factor for liquid iron at a density of 6.862 g/cc and temperature of 1893 K. Circles are from Ref. 22, and the solid line is theory.

Fig. 7. Shear viscosity for liquid iron as a function of temperature. Circles are from Ref. 25, and the solid line is theory.

Fig. 8. Theoretical melting curve and shock Hugoniots for iron.

Fig. 9. Shock velocity-particle velocity data for iron at four initial densities. Experimental data are from Refs. 20, 27, and 28, and the solid lines are theory.

Fig. 10. Hugoniot for porous iron having an initial density of 4.8 g/cc. Experimental data are from Refs. 20 and 27. The lower section of the calculated curve corresponds to the solid and the upper section corresponds to the fluid. The mixed phase region is shown by a dashed curve.

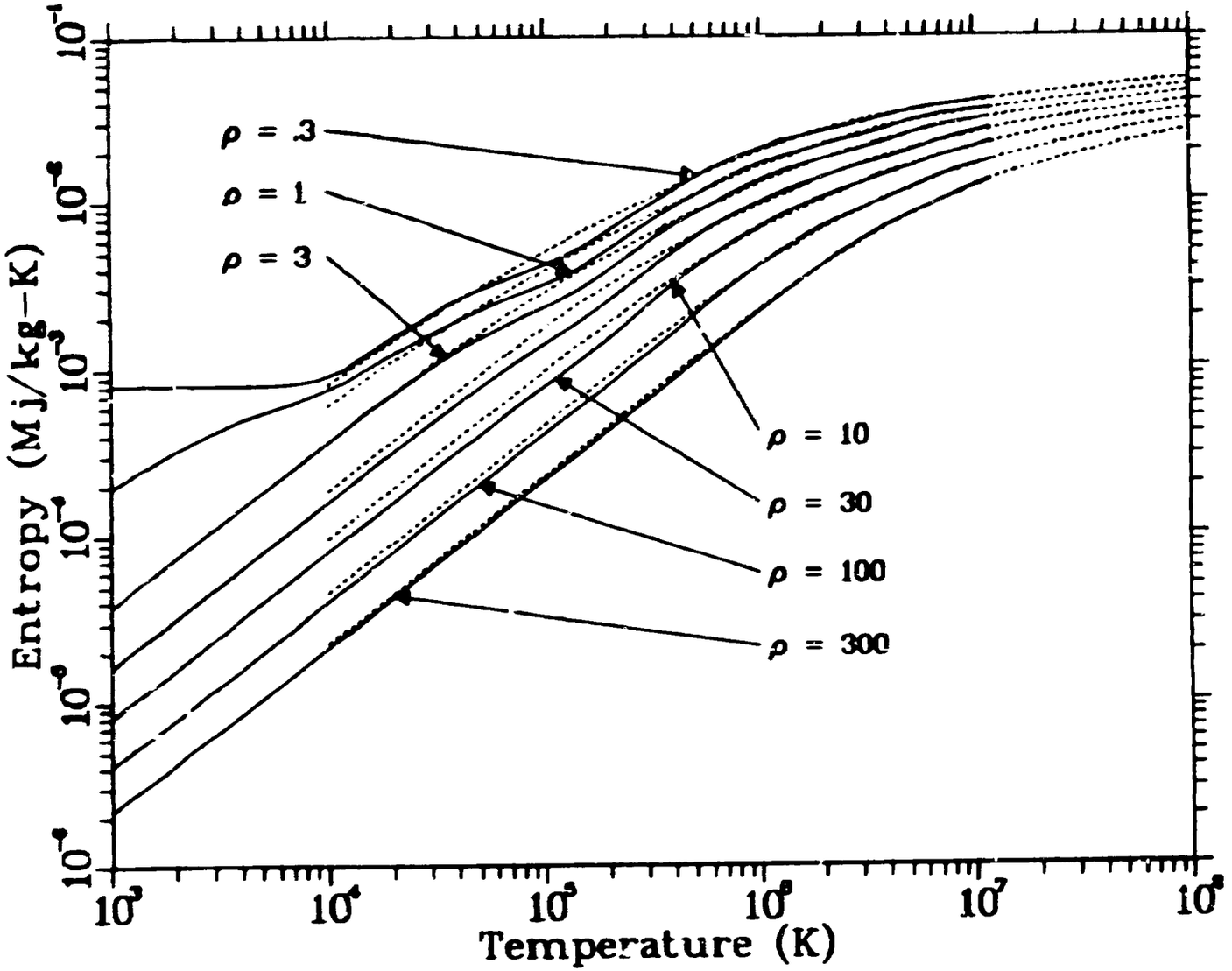
ρ = .3
ρ = 1
ρ = 3
ρ = 10
ρ = 30
ρ = 100
ρ = 300
Entropy (Mj/kg−K)
Temperature (K)

Pressure (GPa)
10^0
10^1
10^2
10^3
4.0
6.0
8.0
10.0
12.0
14.0
16.0
18.0
20.0
22.0
24.0
26.0
Density (g/cc)

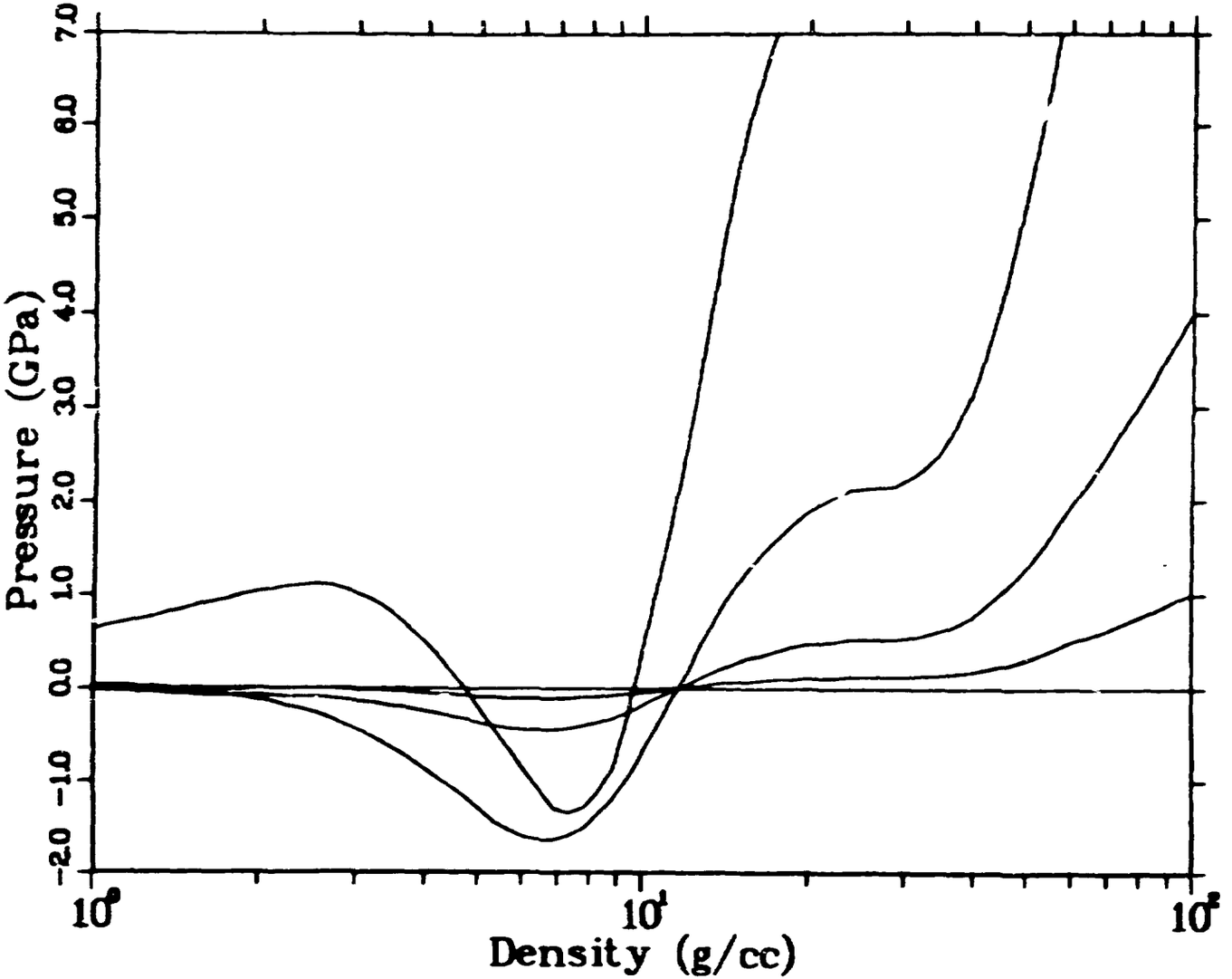
Pressure (GPa)
7.0
6.0
5.0
4.0
3.0
2.0
1.0
0.0
-1.0
-2.0
10⁰
10¹
10²
Density (g/cc)

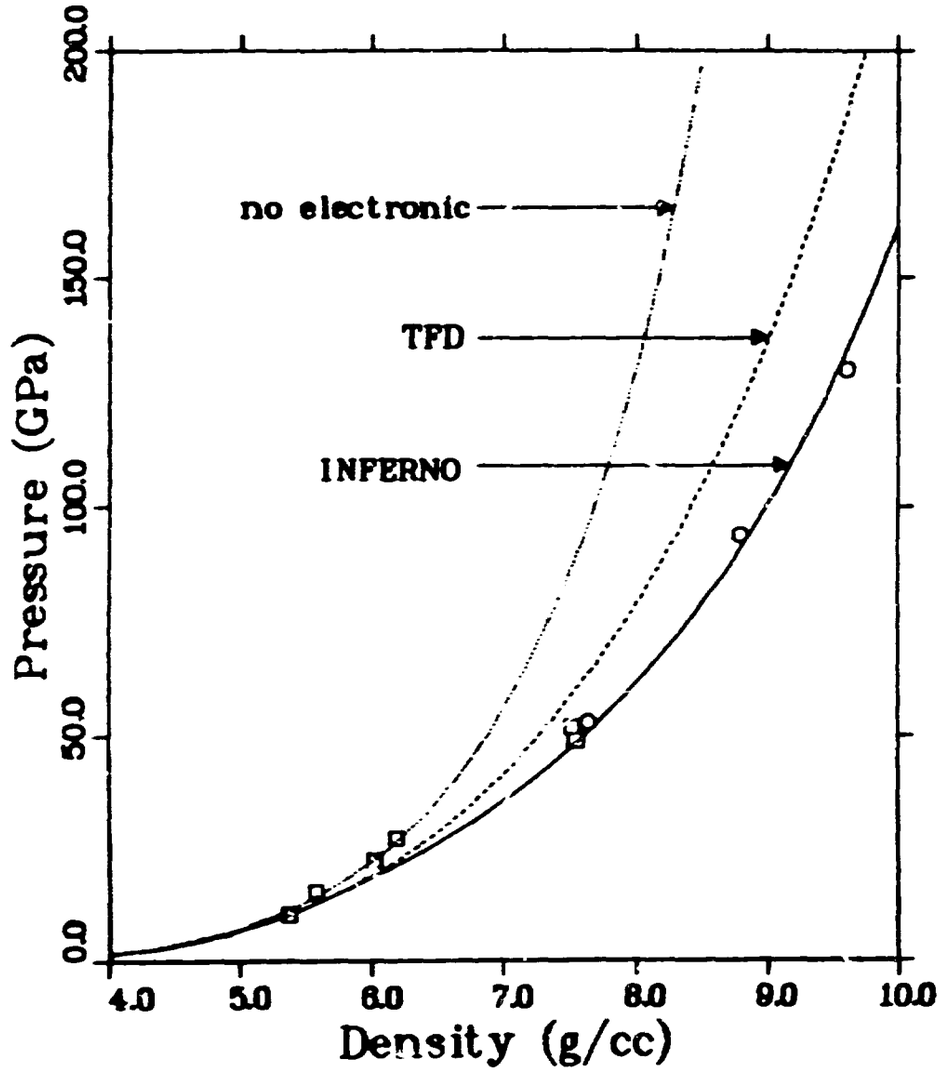
no electronic
TFD
INFERNO
Pressure (GPa)
0.0
50.0
100.0
150.0
200.0
4.0
5.0
6.0
7.0
8.0
9.0
10.0
Density (g/cc)

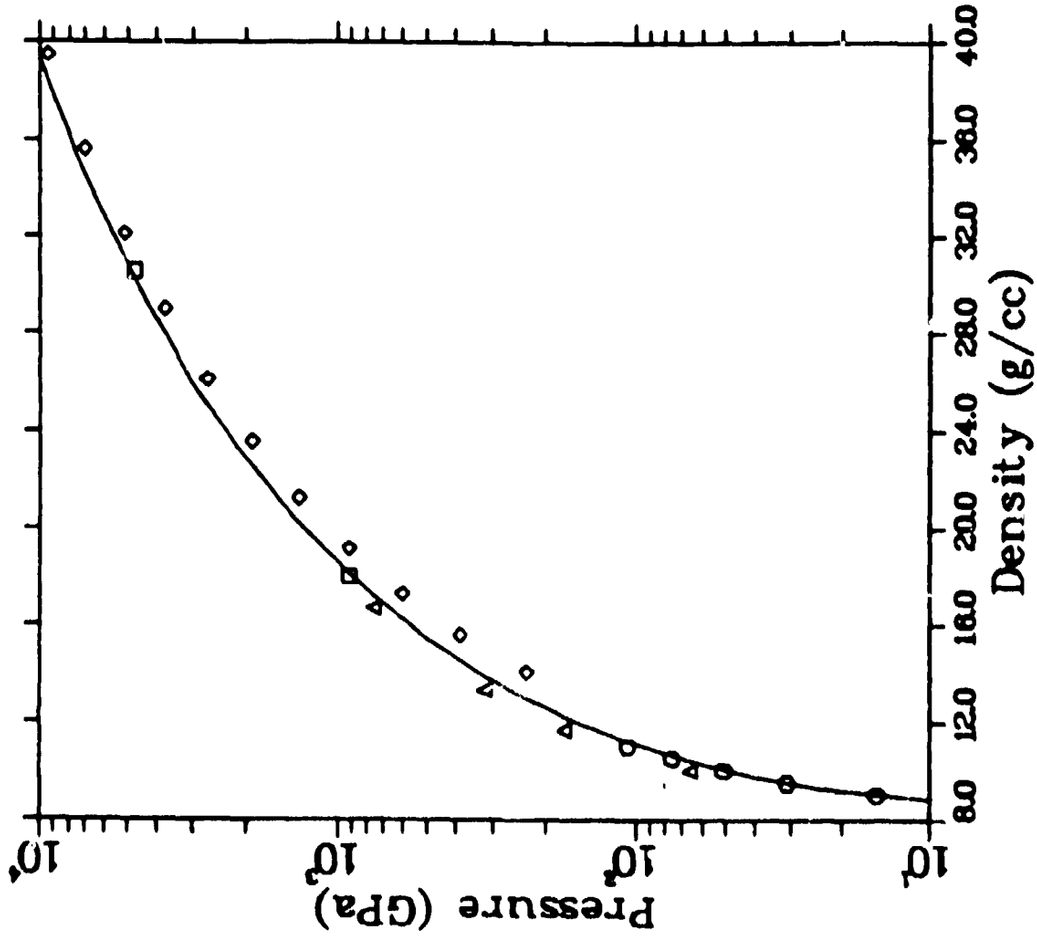

FIG. 5 - G. I. KERLEY - "THEORETICAL MODEL OF LIQUID METALS"

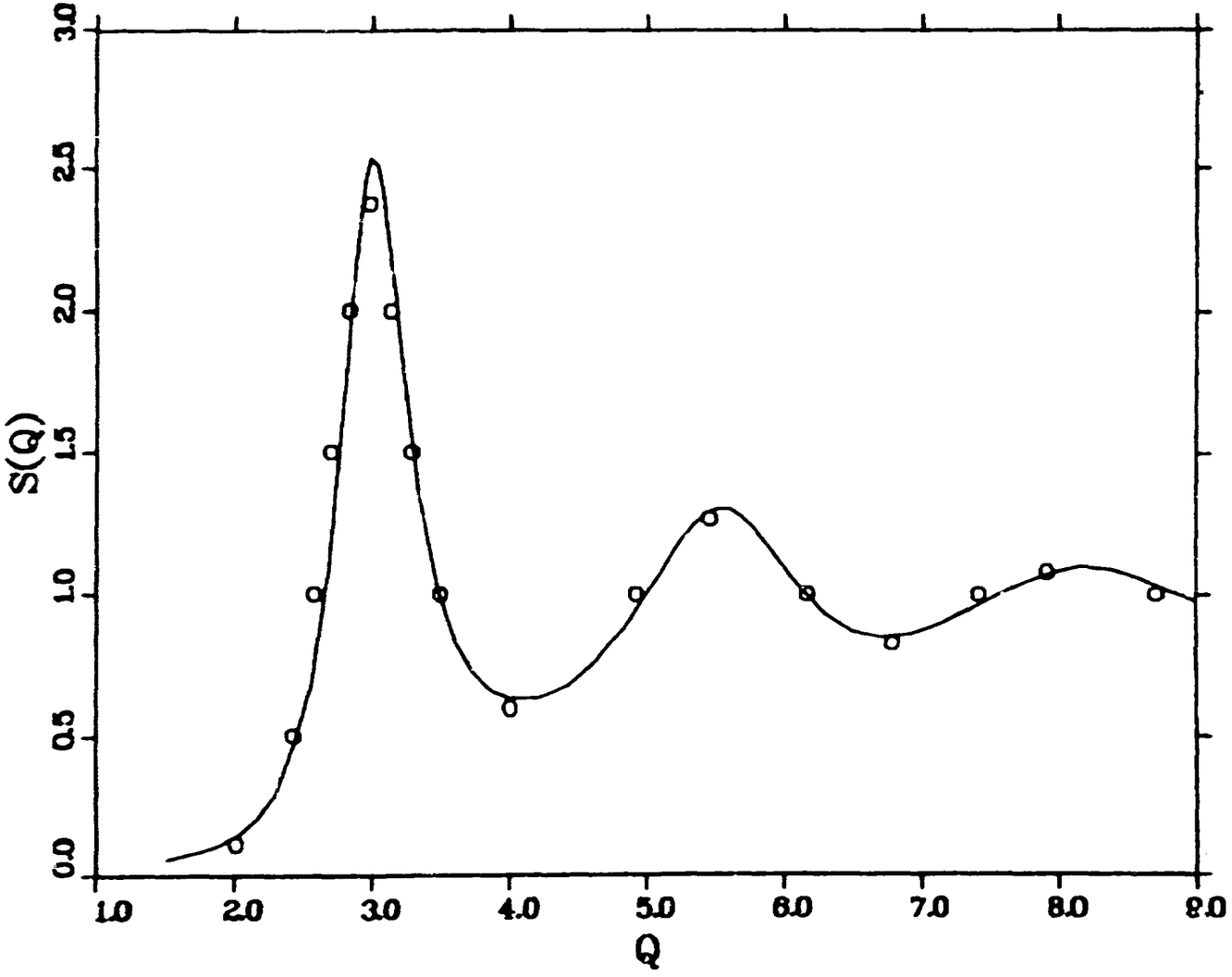
S(Q)
Q
0.0
0.5
1.0
1.5
2.0
2.5
3.0
1.0
2.0
3.0
4.0
5.0
6.0
7.0
8.0

Shear Viscosity (Poise)
0.025
0.030
0.035
0.040
0.045
0.050
0.055
1700.0
1800.0
1900.0
2000.0
2100.0
2200.0
2300.0
2400.0
2500.0
Temperature (K)

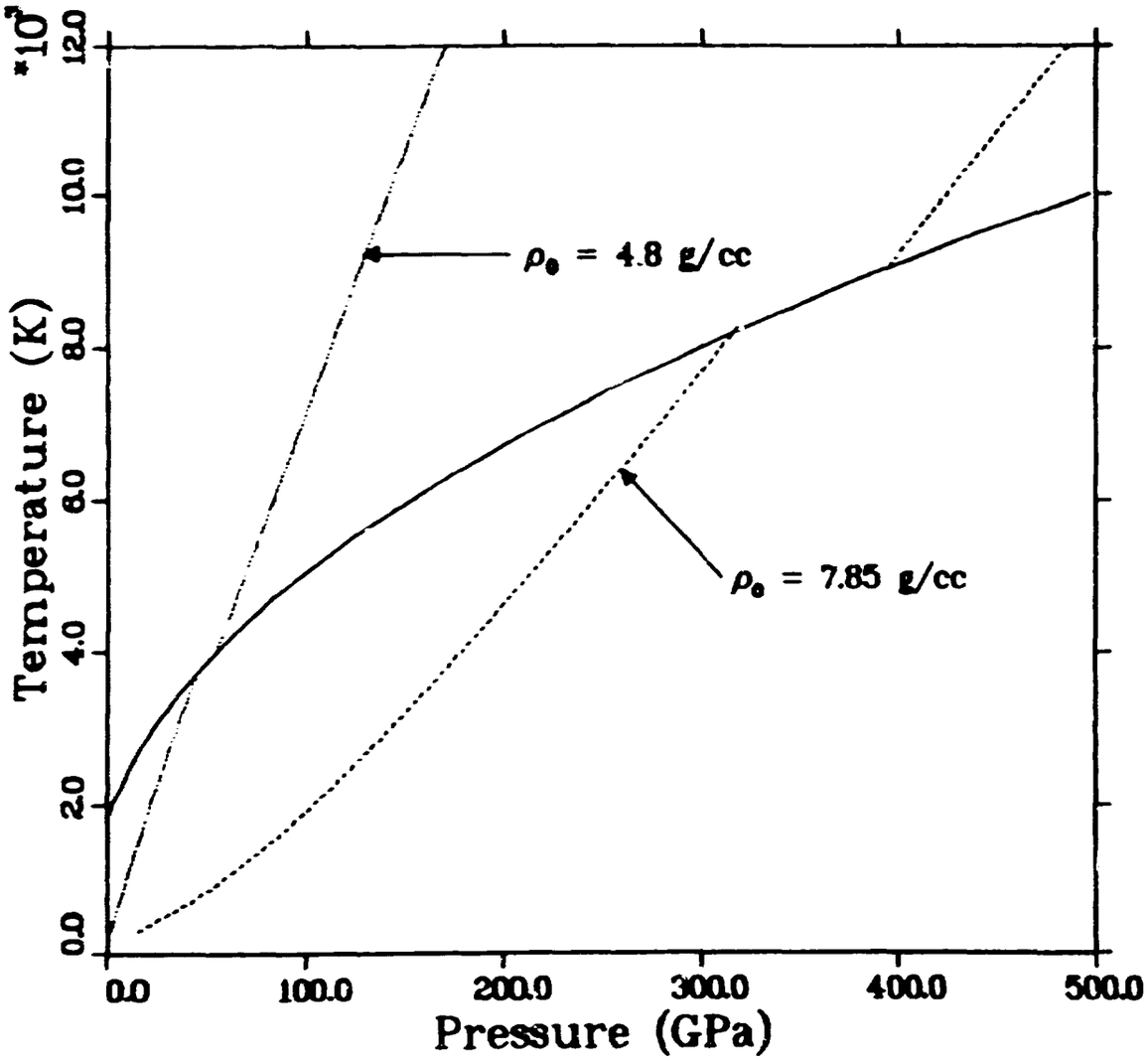
*10³
12.0
10.0
8.0
6.0
4.0
2.0
0.0
Temperature (K)
ρ_0 = 4.8 g/cc
ρ_0 = 7.85 g/cc
0.0
100.0
200.0
300.0
400.0
500.0
Pressure (GPa)

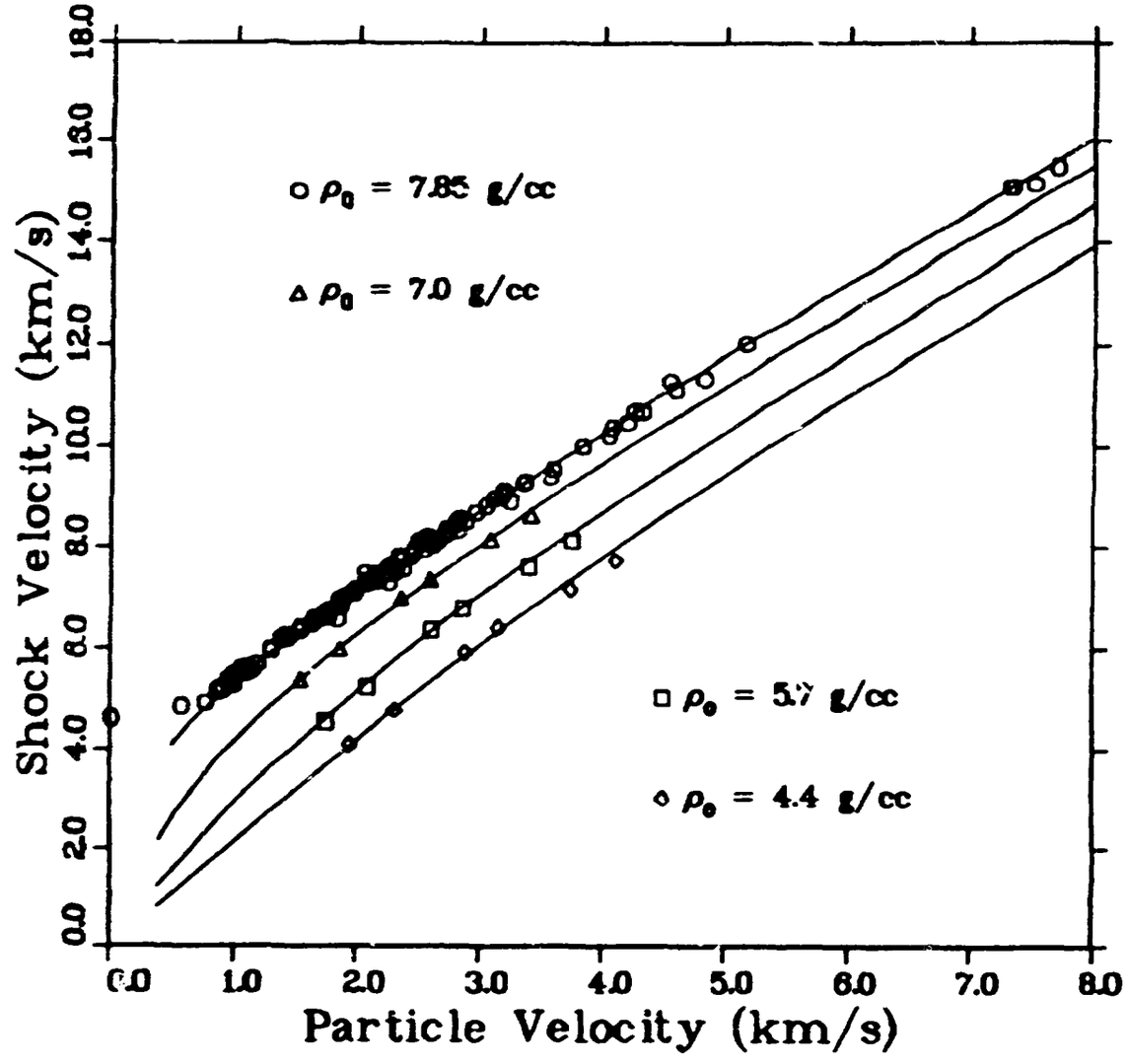
Shock Velocity (km/s)
Particle Velocity (km/s)
0.0
2.0
4.0
6.0
8.0
10.0
12.0
14.0
16.0
18.0
1.0
3.0
5.0
7.0
o ρ_0 = 7.85 g/cc
Δ ρ_0 = 7.0 g/cc
□ ρ_0 = 5.7 g/cc
◇ ρ_0 = 4.4 g/cc

FIG. 10. U-u RELATION - "THEORETICAL MODEL OF [illegible]"